TECHNICAL NOTE

ESTIMATION OF LOAD ON CONTROL LINES OF RAM AIR PARACHUTE DESIGNED FOR PRECISE DELIVERY USING 9-DOF MODEL

Balraj Gupta, Vipin Kumar and Ravi Krishna
Aerial Delivery Research and Development Establishment (ADRDE)
Defence Research and Developmet Organisation (DRDO)
PB No 51, Station Road, Agra Cantt - 282 001, India
Emails : directoradrde@dataone.in; aerovipin@gmail.com

S.C. Upadhyaya
Department of Optical Instrumentation
DDIVE, Dr BR Ambedkar University
Agra - 282 001, India

A.K. Ghosh
Department of Aerospace Engineering
Indian Institute of Technology Kanpur
Kanpur - 208 016, India

Abstract

Controlled Aerial Delivery System (CADS) consists of Ram Air Parachute (RAP) Airborne Guidance Unit (AGU) and useful payload. AGU pulls the control lines attached to the control surfaces of RAP and provides required maneuverability to the system. Estimation of load on control lines is essential for design and development of Airborne Guidance Unit (AGU). This paper presents the mathematical methods of the estimation of load on control lines the results of which are validated by experiments. The mathematical estimate of the load on control lines was carried out by developing a model similar to the aircraft control surface hinge moment estimation. The mathematical model was incorporated in 9DOF model to arrive at real time load estimation on control lines during inflation and subsequent steady flight condition. Experimental results are obtained during flight trials by using load cells on control lines and current sensor on power line of actuators. The mathematical results are in good agreement with the experimental results. The load on control lines are within 6 to 8% of the suspended load.

***Key Words**: Ram air parachute, 9DOF, Flap deflection*

Nomenclature

9-DOF	= Nine Degree of Freedom
AR	= Aspect ratio of parafoil
AGU	= Airborne Guidance Unit
b	= Canopy span
C_D	= Drag coefficient
C_L	= Lift coefficient
C_Y	= Side force coefficient
$C_{h\alpha}$	= Alpha derivatives of hinge moment coefficient
$C_{h\delta}$	= Delta derivatives of hinge moment coefficient
CADS	= Control Aerial Delivery System
c	= Canopy chord length
c_f	= Control surface chord length
D	= Drag force
d	= Diameter of link
e	= Oswald efficiency factor
F	= Force
g	= Acceleration due to gravity
L	= Lift force
m	= Mass
q	= Dynamic pressure
RAP	= Ram Air Parachute

Paper Code : V63 N2/726-2011. Manuscript received on 26 July 2010. Reviewed and accepted as a Technical Note on 23 Sep 2010

Introduction

Airdrop technology is a vital capability for rapid deployment of payloads to specific rendezvous points. To produce rapidly deployable units, there is a driving need to equip individual payload package with a parachute and guidance and control module so that each system can steer itself to a pre-specified rendezvous point after release from delivery aircraft. RAP with their abilities of gliding and maneuverability are occupying the prominent place in airdrop technology as an alternative to round canopy parachutes. The CADS shown in Fig.1 with its AGU steers its flight path toward predetermined target by operating two control lines of RAP. Maneuvering of RAP is achieved by asymmetrical deflection of control surfaces. This deflection creates both yawing and rolling moments. However, symmetrical deflection of control surfaces is required for controlling the speed of RAP and also for flare landing.

The investigation of stability, opening phenomena and flight performance of RAP has done by many researchers but limited attention is made in load on control line of RAP e.g. Walker [1] investigated the static and dynamic stability of ram air parachute using a model mounted horizontally in a wind tunnel. The model was supported on pivoted rods which represented suspension lines. Sobieski [2] derived details aerodynamics of ram-air parachute. He explained the comparison of flow characteristic over airfoil and parafoil canopy. He has explained the source of lift from the Bernoulli's equation. He has demonstrated how aerodynamic forces and moment work on ram air parachute. Lingard [3] clearly mentioned three things, first, too high rigging angle result in performance loss, where too low rigging angle results in trim angle of incident beyond stall. Second, increased aspect ratio results in increased static stability. Third, longer line length results in increased static stability and increased sensitivity to rigging. The expression for lift and drag coefficient were first derived by the Lingard [4].The parafoil was called ram air parachute throughout his report. He has also modified the expressions for wing having anhedral. The effect of type of parafoil, size of parafoil, and wind velocity on performance has been addressed. The equation of motion of gliding parafoil has been derived. The longitudinal stability by deriving the moment equation for parafoil payload system has been simulated and it has discussed the effect of line length on longitudinal performance. The trim angle of attack depends on the rigging angle. It has been concluded that longer line length requires increased rigging angle to attain desired trim lift coefficient. Finally he concluded that at small line length there is a small change in trim angle of attack where lift and drag coefficient increase in proportion resulting in reduced lift drag ratio. Peyada et al. [5] attempts to formulate the flight dynamics model for parafoil-payload system by including the analytically derived expression of stability derivative (at high angle of attack) in 9 DOF equation motion. Iosilevskii [6] analyzed detail longitudinal stability and control of gliding parachute. He first gave the expression for pitching moment. He has shown that, the most forward centre of gravity (c.g.) position is limited by a loss of longitudinal static stability and by a loss of control power, where the most rear c.g. position is limited by a requirement of stall-free controls range. Ultimately he has given various conditions and expressions for forward and backward c.g. limits. Slegers and Costello [7] described mathematical model of 9 DOF parafoil-payload systems. The parafoil system is modeled as rigid parafoil and rigid store that are connected to each other by rigid suspension lines and a riser. Included in the riser is a hinge that allows free three axes rotation of the parafoil with respect to the joint point and it transfers forces and moment in yaw only. The hinge is modeled as a damped spring. Prakash and Ananthkrishnan [8] optimized the rigging angle to obtain good glide as well as good flare characteristics at different symmetric brake deflection using bifurcation analysis for parafoil-payload system. They used 9 DOF model to carryout dynamic simulations for open loop, and closed loop with designed yaw controller. Berland et al. [9] presented the derived load for control line deflection based on current and voltage monitoring of motor during flight test. Nathan Slegers et al. [10] investigate control issues for a parafoil and payload system with left and right parafoil brakes used as the control mechanism. It is shown that parafoil and payload systems can exhibit two basic modes of lateral control, namely, roll and skid steering. These two modes of lateral steering generate lateral response in opposite directions.

The object of the present work is to developed mathematical model for estimation of load experienced by control lines the effect of which is felt on AGU. The results are in turn validated by using sensors during actual flight trials.

Mathematical Modeling of Ram Air Parachute with Payload

The parafoil-payload system is modeled as a two-body system consisting of canopy mass (including apparent mass and included air mass) and rigid payload mass suspended below the canopy through suspension lines. The

suspension lines are attached to the payload riser through connection point allowing independent rotational motion of canopy and payload. Thus parafoil-payload system requires 9DOF flight dynamics model which includes 3-translational motion and 3-rotational motion each of parafoil and payload.

Modeling Assumptions

- The parafoil system consists of two rigid masses.
- The rigid mass less links connects parafoil canopy and payload to joint C, respectively.
- The joint C allows free rotation of canopy and payload about itself.
- The joint is considered to transfer only forces but no moments.
- Apparent mass center of parafoil is taken to be same as rigid canopy mass center.

Reference Frames

Derivation of 9-DOF equations of motion uses the following Right-handed Cartesian reference frames as illustrated in Fig.2.

- Joint point O fixed reference frame, X_o, Y_o, Z_o.
- Parafoil canopy fixed reference frame, X_P, Y_P, Z_P at the CG of parafoil.
- Payload body fixed reference frame, X_L, Y_L, Z_L, at the CG of load.

In joint point O fixed reference frame, the X_o axis points forward, parallel to Earth horizontal. The Z_o axis is pointing downward and perpendicular to X_o. The Y_o axis is perpendicular both X_o and Z_o. This frame has a translational velocity $V_o(u_o, v_o, w_o)$, but has no angular rotation with respect to Earth fixed axis (X_e, Y_e, Z_e). The X_P axis of parafoil canopy fixed reference frame points forward, parallel to the canopy baseline (or chord) in the plane of symmetry. The Z_P axis points downward and perpendicular to span wise plane of symmetry. The Y_P axis is normal to XZ plane of parafoil to form a right-handed axis system. In this axis system, the canopy mass centre has translation velocity $V_p(u_p, v_p, w_p)$, angular velocity $\Omega_p(p_p, q_p, r_p)$, and angular orientation angles (or Euler angles) $\varphi_p, \theta_p, \psi_p$. The X_L axis of payload body reference frame points forward normal to the connecting link between joint point O and payload CG. The Z_L axis points downward, parallel to the link. The Y_L axis is normal to the X_L and Z_L axes according to right-hand rule. In this reference frame the payload mass centre has translation velocity $V_L(u_L, v_L, w_L)$, angular velocity $\Omega_L(p_L, q_L, r_L)$ and Euler orientation angles $\varphi_L, \theta_L, \psi_L$ with respect to the joint point reference frame. The velocity vector at parafoil CG (V_p) and payload CG (V_L) on parafoil and payload reference frame respectively with respect to joint point reference frame are derived as

$$V_P = C_P V_o + \Omega_p \times l_{SP} \qquad V_L = C_L V_o + \Omega_L \times l_{SL} \tag{1}$$

The transformation matrix C_P and C_L are related by the three Euler angle Ω_P, θ_P, φ_P and Ω_L, θ_L, φ_L respectively.

$$C_P = \begin{bmatrix} \cos\theta_P \cos\psi_P & \cos\theta_P \sin\psi_P & -\sin\phi_P \\ \sin\phi_P \sin\theta_P \cos\psi_P - \cos\phi_P \sin\psi_P & \sin\phi_P \sin\theta_P \sin\psi_P + \cos\phi_P \cos\psi_P & -\sin\phi_P \cos\theta_P \\ \cos\phi_P \sin\theta_P \cos\psi_P + \sin\phi_P \sin\psi_P & \cos\phi_P \sin\theta_P \sin\psi_P - \sin\phi_P \cos\psi_P & \cos\phi_P \cos\theta_P \end{bmatrix} \tag{2}$$

$$C_L = \begin{bmatrix} \cos\theta_L \cos\psi_L & \cos\theta_L \sin\psi_L & -\sin\phi_L \\ \sin\phi_L \sin\theta_L \cos\psi_L - \cos\phi_L \sin\psi_L & \sin\phi_L \sin\theta_L \sin\psi_L + \cos\phi_L \cos\psi_L & -\sin\phi_L \cos\theta_L \\ \cos\phi_L \sin\theta_L \cos\psi_L + \sin\phi_L \sin\psi_L & \cos\phi_L \sin\theta_L \sin\psi_L - \sin\phi_L \cos\psi_L & \cos\phi_L \cos\theta_L \end{bmatrix} \tag{3}$$

The Time derivative of the Euler angle are related to the fixed components of the angular velocity vector (p, q, r).

$$\begin{bmatrix} \dot{\phi}_P \\ \dot{\theta}_P \\ \dot{\psi}_P \end{bmatrix} = \begin{bmatrix} 1 & \sin\phi_P \tan\theta_P & \cos\phi_P \tan\theta_P \\ 0 & \cos\phi_P & -\sin\phi_P \\ 0 & \sin\phi_P \sec\theta_P & \cos\phi_P \sec\theta_P \end{bmatrix} \begin{bmatrix} p_p \\ q_p \\ r_p \end{bmatrix} \tag{4}$$

$$\begin{bmatrix} \dot{\phi}_L \\ \dot{\theta}_L \\ \dot{\psi}_L \end{bmatrix} = \begin{bmatrix} 1 & \sin\phi_L \tan\theta_L & \cos\phi_L \tan\theta_L \\ 0 & \cos\phi_L & -\sin\phi_L \\ 0 & \sin\phi_L \sec\theta_L & \cos\phi_L \sec\theta_L \end{bmatrix} \begin{bmatrix} p_L \\ q_L \\ r_L \end{bmatrix} \tag{5}$$

The motion of the system is expressed by the translation velocity V_0 and by the angular velocity of parafoil, Ω_P and of the load relative to earth-fixed coordinates. This leads to 18 independent kinematics variables corresponding to the 9 DOF of the system.

Trajectory of the Connection Point O

The velocity vector V_0 on Earth-parallel coordinate provides three differential equations for the trajectory of the connecting point O

$$\begin{bmatrix} \dot{X}_e \\ \dot{Y}_e \\ \dot{Z}_e \end{bmatrix} = \begin{bmatrix} \dot{X}_o \\ \dot{Y}_o \\ \dot{Z}_o \end{bmatrix} = V_o \tag{6}$$

9-DOF Equations of Motion

The connection point O has been selected as a reference point instead of the centre of gravity of the system. So, six more differential equations are derived from the equation of motion, based on the equilibrium of forces and moments, which act on the parafoil-load system [13].

Equilibrium of forces

Forces acting at the payload center

$$m_L C_L V_o + m_L \Omega_L \times l_{SL} + m_L \Omega_L \times (\Omega_L \times l_{SL}) = F_L^A + F_L^g - F_L^o \tag{7}$$

Where,

$$F_L^A = \frac{1}{2} \rho V_L S_L \begin{Bmatrix} u_L C_D^L \\ v_L C_D^L \\ w_L C_D^L \end{Bmatrix};$$

$$F_L^g = m_L g \begin{Bmatrix} -\sin\theta_L \\ \sin\varphi_L \cos\theta_L \\ \cos\varphi_L \cos\theta_L \end{Bmatrix}; \; F_L^o = C_L F_o \tag{8}$$

Forces acting at the parafoil center

$$(m_P + m_{PA}) C_P V_o + (m_P + m_{PA}) \Omega_P \times l_{SP} - m_{PA} \Omega_{PA} \times C_P V_o$$

$$+ \Omega_P \times m_{PA} C_P V_o + \Omega_P \times (m_P + m_{PA}) \Omega_P \times l_{SP} = F_P^A + F_P^g + F_P^o \tag{9}$$

Where,

$$F_P^A = \frac{1}{2} \rho V_P S_P \begin{Bmatrix} C_X \\ C_Y \\ C_Z \end{Bmatrix};$$

$$F_P^g = m_P g \begin{Bmatrix} -\sin\theta_P \\ \sin\varphi_P \cos\theta_P \\ \cos\varphi_P \cos\theta_P \end{Bmatrix}; \; F_P^o = C_P F_o \tag{10}$$

Equilibrium of moment

Moment acting about payload centre

$$I_L \Omega_L + \Omega_L \times (I_L \Omega_L) = l_{SL} F_L^o \tag{11}$$

Moment acting about payload centre

$$(I_P + I_{PA}) \Omega_L + \Omega_P \times (I_P + I_{PA}) \Omega_P = M_P^A - l_{SL} F_P^o \tag{12}$$

Where aerodynamic moment of parafoil is:

$$M_P^A = \bar{q}_P S_P \begin{Bmatrix} b\,C_l \\ c\,C_m \\ b\,C_n \end{Bmatrix} \quad (13)$$

Apparent Mass of the Parafoil

Apparent mass has a strong effect on the flight dynamics of lightly-loaded flight vehicle such as parafoil. The calculation of these effects are outlined in Lissman and Brown [11], are shown in Eqs. (14) and (15).

$$m_x = 0.666\left(1+\frac{8}{3}a^{-2}\right)\rho\, t^2\, b$$

$$m_y\ 0.267\left(t^{-2}+2\,a^{-2}(1-t^{-2})\right)\rho\, t^2\, c$$

$$m_x\ 0.785\left(1+2\,a^{-2}(1-t^{-2})\right)^{1/2}\frac{AR}{1+AR}\rho\, b\, c^2 \quad (14)$$

$$I_A = 0.055\frac{AR}{1+AR}\rho\, b^3\, S^2$$

$$I_B = 0.0308\frac{AR}{1+AR}\left(1+\frac{\pi}{6}(1+AR)\,AR\,a^{-2}t^{-2}\right)\rho\, c^2\, S$$

$$I_c = 0.0555\left(1+8\,a^{-2}\right)\rho\, b^3\, t^2 \quad (15)$$

The included mass of air 2bctρ and the moment of inertia of the included mass of the parafoil also need to be added with the apparent mass and apparent moment of inertia of the parafoil.

Aerodynamic Model

The postulation of correct aerodynamic model is of paramount importance to develop accurate flight dynamic model of a vehicle. The vehicle considered in the present study consisted of a parafoil, payload and connecting cables called support length. The aerodynamic forces acting on the parafoil are modeled using conventional definition of longitudinal and lateral directional forces and moments. The lift (L), drag (D), side force (F_y), pitching moment (M_y), rolling moment (M_x) and yawing moment (M_z) are modeled as follow:

$$L = q\,S\,C_L \quad ; \quad D = q\,S\,C_D$$

$$F_y = q\,S\,C_y \quad ; \quad M_y = q\,S\,C_m$$

$$M_x = q\,S\,C_l \quad ; \quad M_z = q\,S\,C_n \quad (16)$$

Since parafoil has anhedral angle and generally encounters fairly high angle of attack at trim on flare transition, it is important to model the effect of angle of attack on longitudinal and lateral-directional forces and moments. Fairly exhaustive longitudinal aerodynamic model for parafoil-payload system has been presented in Refs. [4, 12 and 13]. The coefficient of side force, rolling moment and yawing moment can be presented in terms of stability derivatives as:

$$C_y = C_{y_\beta}\beta + C_{y_r}(rb/2V) + C_{y_{\delta_{ab}}}\delta_{ab}$$

$$C_l = C_{l_p}(pb/2V) + C_{l_r}(rb/2V) + C_{l_{\delta_{ab}}}\delta_{ab}$$

$$C_n = C_{n_p}(pb/2V) + C_{n_r}(rb/2V) + C_{n_{\delta_{ab}}}\delta_{ab} \quad (17)$$

Dependencies of Stability Derivatives on Angle of Attack

Peyada et. al [10] has shown dependencies of Stability derivatives on angle of attack and derived expressions for Longitudinal and Lateral-Directional Stability derivatives which are reiterated below:

$$C_{Y\beta} = \left[C_L\sin(\alpha) - C_{L\alpha}\cos(\alpha) - C_D\cos(\alpha) - C_{D\alpha}\sin(\alpha)\right]\Gamma^2 - C_{D_{Ram}} \quad (18)$$

$$C_{l\beta} = \left[-C_L\sin(\alpha) + C_{L\alpha}\cos(\alpha) + C_D\cos(\alpha) + C_{D\alpha}\sin(\alpha)\right]\frac{\Gamma}{4} \quad (19)$$

$$C_{n\beta} = C_{D_{Ram}} * 0.5c/b + \left[C_L\cos(\alpha) + C_{L\alpha}\sin(\alpha) + C_D\sin(\alpha) - C_{D\alpha}\sin(\alpha)\right]\frac{\Gamma}{4}$$
$$+\left[C_L\sin(\alpha) - C_{L\alpha}\cos(\alpha) - C_D\cos(\alpha) - C_{D\alpha}\sin(\alpha)\right]\Gamma^2\,(0.25c/b) \quad (20)$$

$$C_{lp} = \left[C_L\sin(\alpha) - C_{L\alpha}\cos(\alpha) - C_D\cos(\alpha) - C_{D\alpha}\sin(\alpha)\right]/8 \quad (21)$$

$$C_{np} = \left\{(\Gamma c/8b)\left\{-C_L\sin(\alpha) + C_{L\alpha}\cos(\alpha) + C_D\cos(\alpha) + C_{D\alpha}\sin(\alpha)\right\}\right.$$
$$\left. - \left\{C_L\cos(\alpha) + C_{L\alpha}\sin(\alpha) - C_D\sin(\alpha) - C_{D\alpha}\sin(\alpha)\right\}\right/8 \quad (22)$$

$$C_{lr} = \left[C_L\cos(\alpha) + C_D\sin(\alpha)\right]/4 \quad (23)$$

$$C_{nr} = \left[C_L\sin(\alpha) - C_D\cos(\alpha)\right]/4 - \left[C_L\cos(\alpha) + C_D\sin(\alpha)\right]\,(0.25\,\Gamma\, c/b) \quad (24)$$

Analytical Method for Estimation of Loads on Control Line

The analytical method formulation for the estimation of load on control line that has been used here is similar to the aircraft hinge moment calculation. The control surface load can be approximated if hinge moment coefficient is known. The hinge moment coefficient for a flap can be approximated as follows:

$$C_h = C_{ho} + C_{h\alpha}\,\alpha + C_{h\delta}\,\delta \tag{25}$$

where,

$$C_{ho} = C_{Lo} \times \frac{x}{c}$$

$$C_{h\delta} = C_{L\alpha} \times \tau \times \frac{x}{c}$$

$$C_{ha} = C_{h\delta} \times \left(1 - \frac{\partial \varepsilon}{\partial \alpha}\right)$$

$$\frac{\partial \varepsilon}{\partial \alpha} = \frac{2\,C_{L\alpha}}{\pi\,AR} \tag{26}$$

$\tau = 0.5$ is obtained for Control surface area/Lifting surface area = 0.25, from Refs.[15], and $C_{L\alpha}$ for finite wing is estimated by:

$$C_{L\alpha} = \frac{C_{l\alpha}}{1 + \dfrac{C_{l\alpha}}{\pi\,e\,AR}} \tag{27}$$

Hinge moment (shown in Fig.3) acting on single flap is obtained as:

$$H_M = C_h \times \frac{1}{2}\rho\,V^2\,S_f c_f \tag{28}$$

Therefore, Load on control line is estimated as:

$$F_{control} = \frac{H_M}{c_f} \tag{29}$$

The present work attempts to formulate the aerodynamic model for parafoil payload system is described using Eqs. (1) to (15) using proposed analytically derived expression (Eqs. (25) to (29)) for estimation of load on control line. The equations of motion are solved using Runge-Kutta fourth order scheme for solving simultaneous differential equations. Time step for this integration is selected to be of size 0.001s. The stability derivatives $C_{Y\beta}$, $C_{l\beta}$, $C_{n\beta}$, C_{lp}, C_{np}, C_{lr}, and C_{nr} were estimated using Eqs. (18) to (24) and the valve of C_L and C_D were taken from wind tunnel results.

The loads on control line were estimated for different - different brake conditions and angle of attack, rate of descent (w) and horizontal velocity (u) also are presented in Fig.4. From Fig.4 the maximum load on control lines is 60 kgf = 12% of total suspended weight for 100% of full flap deflection (Port (Pt) = 60 and Starboard (Sb) = 60 deg) and 47 kgf = 9.4% of total suspended weight for 83% flap deflection i.e. Pt = 50 and Sb = 50 deg. Results also shows as flap deflection increases angle of attack increases from 7.5 to 12 deg, horizontal velocity (u) decreases from 16.5 m/s to 12.6 m/s and rate of descent decreased 17.4 m/s to 12.8 m/s.

Experimental Methods for Estimation of Loads on Control Line

Two methods of estimation of loads on control lines experimentally have been used. The first one is the load cell based method in which Load cell are attached in line with the control line which gives the load on control line during flight trial. The second method is the indirect method of estimation of load on control line by measuring the current drawn by the actuator. The two methods are described in the following sections.

Load Cell Based

The load cells were calibrated on ground and then it was mounted on the gland plate of AGU were it was attached to two control lines. With this configuration, trials with different braking configurations were conducted and a load data was generated for 9 cells RAP as shown in Table-1.

Table-1 : Load on Control Line for Different Flap Deflection

Sl. No.	Payload (Kg)	Flap Deflection (%)	Loand on Control Line (kgf)	Percentage of Suspended Payload (%)
1	62	33.3	4.25	6.85
2	62	58.3	5.25	8.47
3	62	83.3	6.5	10.48
4	72	83.3	7.5	10.42

Current Sensor Based

In this method, a current sensor was integrated in power line of actuator. The current sensor generated the current drawn profile of actuators which is directly proportional to the load pulled by actuator/load on control line. Calibration of the sensors was carried out in lab with the help of Actuator test rig. The current profile generated in the flight trial using current sensor is shown below in Fig.5. During flight trial, a maximum of 48° of command was given for which the feedback was 40 which corresponds to 67% of full flap deflection. The peak current drawn by the actuator during this period was 2.3A which corresponds to 48.14 kgf of load which is equal to 9.63% of the suspended payload as shown in Fig.6.

Discussion

The comparison plot of the load on control lines for different flap deflection as obtained by mathematical and experimental methods is shown in Fig.7. The plot shows that the results obtained by the mathematical model incorporated in 9DOF formulation are in close agreement with the experimental results.

Conclusion

The mathematical formulation used for the estimation of load on control lines of RAP similar to aircraft hinge moment calculation seems to be correct. The experimental results also agree with the results obtained from the 9DOF model. Hence, the mathematical model developed for estimation of load on control lines can be used to generate load requirements for the design and development of AGU. Since, the mathematical model is coefficient based, it can be applied to any size of RAP system.

Acknowledgements

The authors acknowledge all the support received from colleagues of different groups in the laboratory specially Mr Manish Bhatnagar, Mr Vikas Bharwaj and Mr Ajeet Gaur.

References

1. Walker, R H., "Static and dYnamic Longitudinal Stability of a Semi Rigid Para-foil", AIAA 70-1191, 1970.

2. Sobieski, J., "The Aerodynamics and Piloting of High Performance Ram-Air Parachute", May, 1994, (http://www.afn.org/skydive/sta/highperf.pdf.).

3. Lingard, J. S., "The Performance and Design of Ram-Air Gliding Parachutes", Precision Aerial Delivery Seminar, Technical Report, Royal Aircraft Establishment, August, 1981.

4. Lingard, J. S., "Ram-air Parachute Design, Precision Aerial Delivery Seminar", 13th AIAA Aerodynamic Decelerator Systems Technology Conference, Clearwater Beach, May, 1995.

5. Peyada, N. K., Ankur Singhal., Ghosh A. K., "Trajectory Modeling of a Parafoil in Motion Using Analytically Derived Stability Derivative at High Angle of Attack", 20th AIAA Aerodynamic Decelerator Systems Technology Conference, Virginia, May, 2007.

6. Iosilevskii, G., "Center of Gravity and Minimal Lift Coefficient Limits of a Gliding Parachute", Journal of Aircraft, Vol. 32, No. 6, pp.1297-1302, 1995.

7. Slegers, N. and Costello, M., "Aspects of Control for a Parafoil and Payload System", Journal of Guidance, Control and Dynamics, Vol.26, No.6, pp. 898-905, 2003.

8. Prakash, O. and Ananthkrishnan, N., "Modeling and Simulation of 9-DOF Parafoil-Payload System Flight Dynamics", AIAA Atmospheric Flight Mechanics Conference and Exhibit, August 21-24, 2006, Keystone, Colorado.

9. Barland J. C., Dunker Storm., George Seam and Barber Justin., "Development of Low Cost 10000 lb Capacity Ram Air Parachute", DRAGFLY Program, AIAA Aerodynamic Decelerator Systems Technology Conference.

10. Nathan Slegers and Mark Costello., "Aspects of Control for a Parafoil and Payload System", Journal of Guidance Control and Dynamics, Vol.26, No.6, November-December, 2003.

11. Lissaman, P. B. S. and Brown, G. J., "Apparent Mass Effects on Parafoil Dynamics", AIAA 93-1236, 12th RAeS/AIAA Aerodynamic Decelerator Systems Technology Conference, 1993.

12. Brown, G. J., "Parafoil Steady Turn Response to Control Input", AIAA Paper 93-1241, May, 1993.

13. Iacomini, C. S. and Cerimele, C. J., "Longitudinal Aerodynamics from a Large Scale Parafoil Test Program", AIAA Paper 99-1732, November, 1999.

14. Etkin, B., "Dynamics of Flight Stability and Control".

15. Nelson, R. C., "Flight Stability and Automatic Control".

16. Raymer, D. P., "Aircraft Conceptual Design", AIAA Educational Series, 1992.

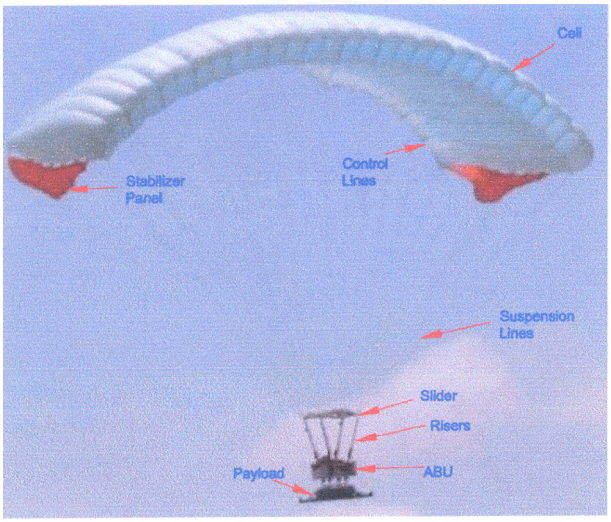

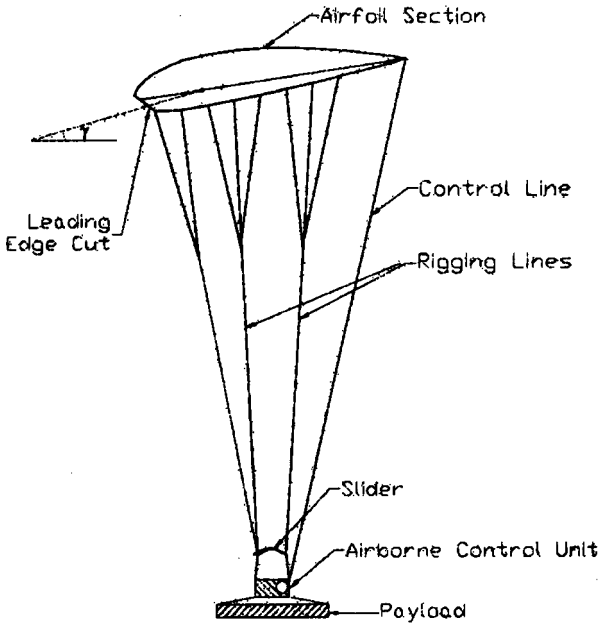

Fig.1 Controlled Aerial Delivery System

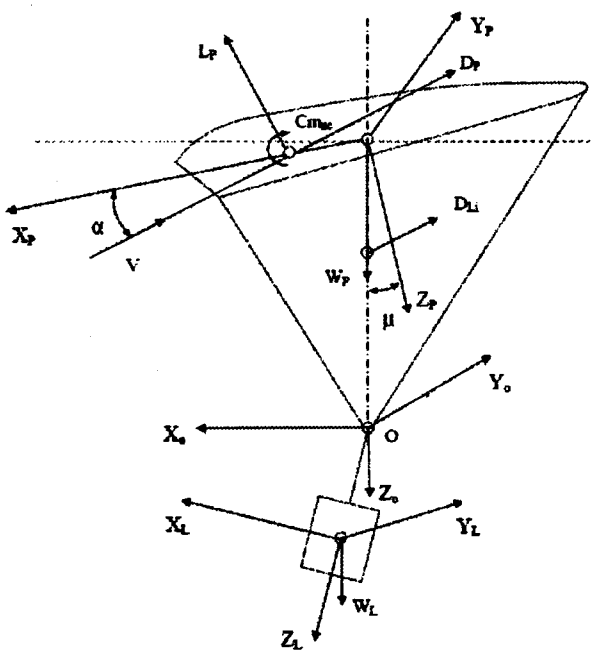

Fig.2 Parafoil Payload System Reference Frames

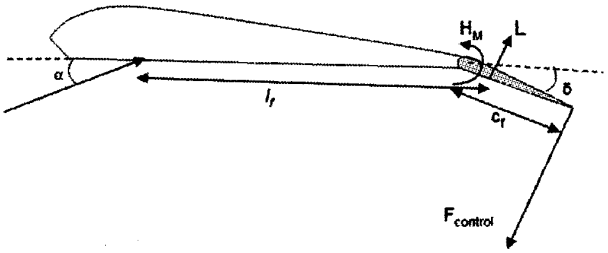

Fig.3 Hinge Moment on Flap and Force on Control Line

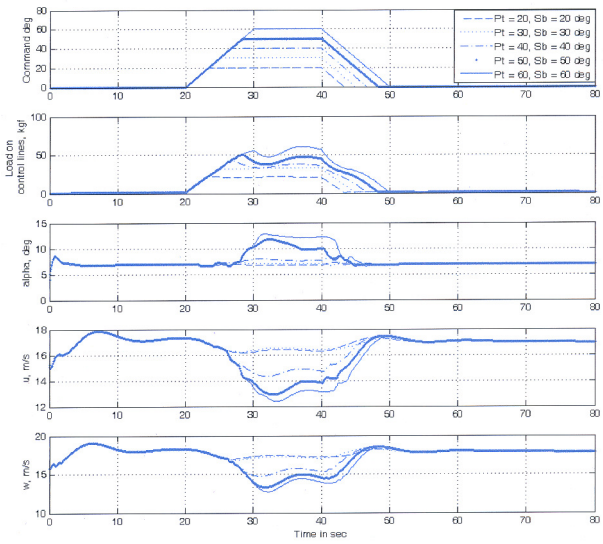

Fig.4 Load on Control Line for Full Flap Deflection for 500 Kg CADS for 6 deg/s of Winding Rate

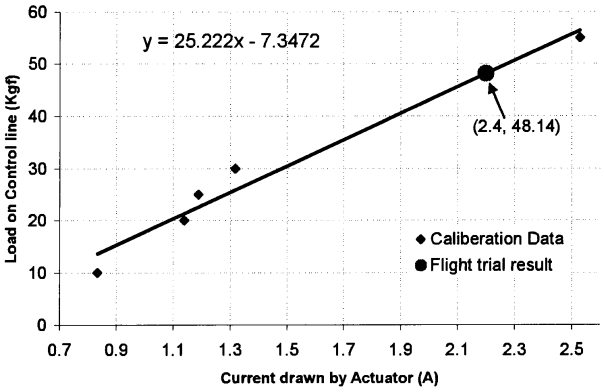

Fig.6 Load on Control Line Versus Current Drawn by Actuator

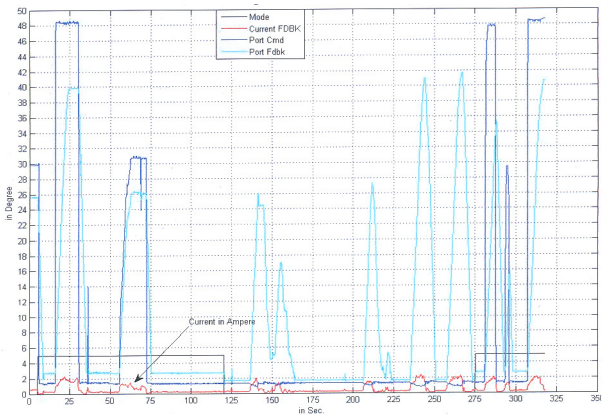

Fig.5 Current Sensor Performance w.r.t. to Control Commands

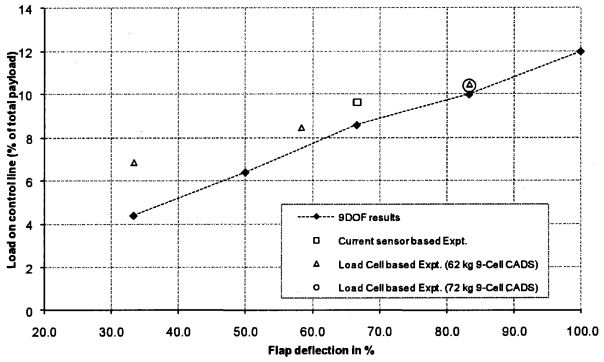

Fig.7 Load on Control Lines as Obtained by Mathematical and Experimental Methods